

Response of non-point source pollutant loads to climate change in the Shitoukoumen reservoir catchment

Lei Zhang · Wenxi Lu · Yonglei An · Di Li ·
Lei Gong

Received: 2 April 2011 / Accepted: 30 August 2011 / Published online: 20 September 2011
© Springer Science+Business Media B.V. 2011

Abstract The impacts of climate change on streamflow and non-point source pollutant loads in the Shitoukoumen reservoir catchment are predicted by combining a general circulation model (HadCM3) with the Soil and Water Assessment Tool (SWAT) hydrological model. A statistical downscaling model was used to generate future local scenarios of meteorological variables such as temperature and precipitation. Then, the downscaled meteorological variables were used as input to the SWAT hydrological model calibrated and validated with observations, and the corresponding changes of future streamflow and non-point source pollutant loads in Shitoukoumen reservoir catchment were simulated and analyzed. Results show that daily temperature increases in three future periods (2010–2039, 2040–2069, and 2070–2099) relative to a baseline of 1961–1990, and the rate of increase is 0.63°C per decade. Annual precipitation also shows an apparent increase of 11 mm per decade. The calibration and validation results showed that the SWAT model was able to simulate well the streamflow and non-point source pollutant loads, with a coefficient of determination of

0.7 and a Nash–Sutcliffe efficiency of about 0.7 for both the calibration and validation periods. The future climate change has a significant impact on streamflow and non-point source pollutant loads. The annual streamflow shows a fluctuating upward trend from 2010 to 2099, with an increase rate of 1.1 m³ s⁻¹ per decade, and a significant upward trend in summer, with an increase rate of 1.32 m³ s⁻¹ per decade. The increase in summer contributes the most to the increase of annual load compared with other seasons. The annual NH₄⁺-N load into Shitoukoumen reservoir shows a significant downward trend with a decrease rate of 40.6 t per decade. The annual TP load shows an insignificant increasing trend, and its change rate is 3.77 t per decade. The results of this analysis provide a scientific basis for effective support of decision makers and strategies of adaptation to climate change.

Keywords Climate change · Shitoukoumen reservoir · Statistical downscaling method · SWAT model · HadCM3 · Non-point source pollution

Introduction

Climate change affects the hydrological cycle and causes increasing atmospheric water vapor content, thereby changing patterns, intensity, and extremes of precipitation, thus changing the runoff over watersheds and the streamflow in rivers. It also modifies

L. Zhang · W. Lu (✉) · Y. An · D. Li · L. Gong
Key Laboratory of Groundwater Resources and
Environment, Ministry of Education,
College of Environment and Resources, Jilin University,
Changchun 130021, China
e-mail: luwenxi@jlu.edu.cn

nutrient transformation and transport characteristics (Murdoch et al. 2000) affecting water quality and exacerbating many forms of water pollution, such as nutrients, sediments, and pathogens, with possible negative impacts on ecosystems and human health (Bates et al. 2008; Campbell et al. 2009; Park et al. 2010; Tu 2009; Williamson et al. 2008). In addition to climate change impacts on water availability and hydrological risks, the consequences to water quality are receiving great attention (Delpla et al. 2009; Hodgkins et al. 2003; Lee et al. 2010; Neff et al. 2000; Yu et al. 2002; Whitehead et al. 2006).

Regional and global climate scenarios and models are useful tools for producing data inputs for hydrological models in order to understand and predict the potential effects of climate change on water bodies (Delpla et al. 2009). Xu (1999) reviewed the methodologies and processes for assessing hydrological responses to global climate change. Among these methodologies, general circulation models (GCMs) are especially important tools for the assessment of climate change and are widely used (Fowler et al. 2007; Ghosh and Mujumdar 2008; Hamlet and Lettenmaier 1999). However, because of their coarse spatial resolution, the outputs from these models may not be used directly in impact studies (Randall et al. 2007). Downscaling and analytical studies can determine the most appropriate GCM for assessing climate change impacts at the watershed scale (Diaz-Nieto and Wilby 2005; Fowler et al. 2007). There are two fundamental techniques for downscaling coarse GCM data to finer resolutions, namely, dynamical downscaling techniques (Graham et al. 2007; Payne et al. 2004; Stone et al. 2001), which involve a nested regional climate model, and statistical downscaling techniques (Chu et al. 2009; Wilby et al. 2002), which employ a statistical relationship between the large-scale climatic state and the local variations derived from historical data. The statistical downscaling technique was applied in the present study.

Hydrologic models are often combined with climate scenarios generated from GCMs to produce potential scenarios of the effects of climate change on water resources and non-point source pollution (Dibike and Coulibaly 2005; Xu 1999). There are mainly four types of hydrological model used to estimate the impact of climate change, namely, empirical models (annual base), water-balance models (monthly base), conceptual lumped-parameter models

(daily base), and process-based distributed-parameter models (hourly or finer base). The choice of a model for a particular case study depends on many factors, the most important being the purpose of the study and model availability. The Soil and Water Assessment Tool (SWAT) includes approaches describing how CO₂ concentration, precipitation, temperature, and humidity affect plant growth, ET, snow, and runoff generation. It has often been used as a tool to investigate climate change effects. During simulation, the climate, land use, soil, topography, and geological variations are all taken into consideration (Arnold and Fohrer 2005). The SWAT model has been applied successfully throughout the world. Arnold and Fohrer (2005) reviewed the background, development, and application of SWAT in many study areas. The SWAT model is a relatively mature model, and therefore, the SWAT model was selected for simulation in the present study. Several case studies of climate change impacts on hydrology and water resources have used a combined GCM–SWAT model system (Grai Prab et al. 2010; Xu et al. 2009; Zhang et al. 2007; Jha 2004; Stone and Hotchkiss 2003; Githui et al. 2009; Limaye et al. 2001). However, little work has been done to examine the effects of future climate changes on agricultural runoff and non-point source pollutant loads.

Shitoukoumen reservoir is a large reservoir at the middle reaches of the Yinma River in a tributary of the Songhua River. It is the main drinking water source of Changchun City. In recent years, the upstream sediments and pollutants from municipal, industrial, and agricultural sources have worsened the water quality and water resources of the Shitoukoumen reservoir, threatening the safety of drinking water for residents in Changchun and the Songhua River water quality. However, the control of non-point source pollution is difficult because the pollution is affected by rainfall runoff, which has great temporal and spatial variations. Therefore, the main objectives of the present study were to evaluate the effect of climate change on future streamflow volume and non-point source pollutant loads at the inlet of the Shitoukoumen reservoir. SWAT, a physically based, distributed hydrological model, was calibrated and validated by comparing observations and simulation data of streamflow and non-point source pollutant at the outlet of the study area. The HadCM3 model developed at the Hadley Centre in the United Kingdom

was downscaled by the Statistical Downscaling Model (SDSM) technique to generate possible future, local meteorological variables including temperature and precipitation in emission scenarios A2 (medium–high emissions) in this study area. The downscaled data were then used as input to the SWAT model to simulate the corresponding future streamflow and non-point source pollutant loads in the Shitoukoumen reservoir catchment. The results of the study are expected to provide a theoretical basis for local water management authorities to make scientific and rational control measures and response plans.

Materials and methods

Description of the study area

Shitoukoumen Reservoir is located in Jiutai City, Jilin Province (125°45'E, 43°58'N). It is a large reservoir in the middle of the Yinma River, which is the major first-level branch of the Songhuajiang River. It covers an area of 4,944 km². The major basins of the region are the Yinma River, the Shuangyang River, and the Chalu River (Fig. 1). The Shitoukoumen reservoir catchment lies in the North Temperate Zone, with a climate of continental, seasonal, temperate, and semi-humid monsoon.

The location is dry and windy in spring, warm and rainy in summer, dry with early frost and rapid cooling in autumn, and with long, cold, multi-northwest winds in winter. The annual average temperature is 5.3°C. The coldest average temperature is -17.2°C in January, and the hottest average temperature is 23.0°C in July. The annual rainfall is 369.9–667.9 mm, and it is mainly concentrated from May to September, which accounts for 80% of annual precipitation. Annual average evaporation is 1658.1 mm, and the largest values occur from April to June, which accounts for 50% of annual evaporation. Thus, there are often drought and serious water shortages in the study area. In recent years, the water quality of Shitoukoumen reservoir has deteriorated because of non-point source pollutants from upstream from sources such as pesticides, fertilizers, urban sewage, rural domestic garbage, wastewater from industrial and mining enterprises in protected areas, and soil erosion. The deterioration of water quality poses a serious threat to the safety of drinking water for residents



Fig. 1 Location of the study area

in Changchun City and to the water quality of the Songhua River.

GCMs and downscaling methodology

The Hadley Centre’s coupled ocean/atmosphere climate model (HadCM3) was used to construct climate change scenarios. Downscaling of the GCM output to the study area was accomplished using the SDSM (Wilby et al. 2002).

The SDSM uses a multi-linear regression approach, using one or more synoptic-scale predictors (region-scale variables, such as GCM variables) to build a correlation with the predictands (site measured variables, such as daily mean temperature, precipitation). This correlation is calibrated using the National Centers for Environmental Prediction (NCEP)/National Center for Atmospheric Research (NCAR) reanalysis data and observed data for 1961–1975 and validated with data for 1976–1990. The NCEP/NCAR reanalysis data set is a continually updating gridded data set representing the

state of the Earth's atmosphere and incorporating observations and numerical weather prediction model output dating back to 1948. It is a joint product from the NCEP and the NCAR (Wikipedia 2011). The derived relationships were then used to downscale ensembles of the same local variables for the future climate using data supplied by the HadCM3 driven by the A2 emission scenarios for the full period 2010–2100. The characteristics of future climate change were analyzed by using linear regression and Mann–Kendall trend analysis methods (Kendall 1975; Mann 1945) during the 2020s (2010–2039), the 2050s (2040–2069), and the 2080s (2070–2099).

The precipitation and temperature changes that are brought by climate change result in significant influence on the composition and water quality of rivers and lakes. Moreover, changes of rainfall intensity and frequency can affect non-point source pollution, so that it will become more urgent to manage wastewater and water pollution. So, the measured daily mean air temperature and precipitation at Shitoukoumen Reservoir weather station from 1961 to 2000 were selected from the daily observational data of the China Meteorological Administration. There are 23 different atmospheric variables, and these were derived from the daily reanalysis dataset of NCEP/NCAR for 1961–2001 at a scale of 2.5° (long.) \times 2.5° (lat.), as well as outputs of scenarios A2 of HadCM3 from 1961 to 2099, with a spatial resolution of 3.75° (long.) \times 2.5° (lat.) (Chu et al. 2009). First, the NCEP data were interpolated to adjust their resolution to be the same as scenarios A2 of the HadCM3 model, and then all of the data were normalized.

SWAT model

SWAT is a basin-scale, continuous time model that operates on a daily time step and is designed to predict the impact of management on water, sediment, and agricultural chemical yields in ungauged watersheds. The model is physically based, computationally efficient, and capable of continuous simulation over long time periods. Major model components include weather, hydrology, soil temperature and properties, plant growth, nutrients, pesticides, bacteria and pathogens, and land management (Arnold et al. 1998; Neitsch et al. 2005).

The AvSWAT2005 was used in this study, which is provided with an ArcView Geographic Information System interface (Di Luzio et al. 2004). The model divides the simulation area into multiple subwater-

sheds which are then divided into units of unique soil/land use characteristics called hydrological response units (HRUs). The classification of the Shitoukoumen reservoir catchment resulted in 26 sub-basins and 113 HRUs.

In SWAT model, hydrology processes simulated include surface runoff estimated using the SCS curve number or Green–Ampt infiltration equation; percolation modeled with a layered storage routing technique combined with a crack flow model; potential evapotranspiration modeled by the Penman–Monteith methods; snowmelt; transmission losses from streams; and water storage and losses from ponds. Sediment yield is calculated with the Modified Universal Soil Loss Equation (MUSLE). Nutrient outputs, including nitrogen and phosphorus, are estimated by tracking their movements and transformations. The nutrient loads are principally estimated by means of nutrient assimilation by plants and daily nutrient runoff losses. These losses are quantified based on the nutrient concentration in the top soil layer, the MUSLE sediment yield equation, and an enrichment ratio that depends on soil and land use type (Arnold et al. 1998).

There are numerous SWAT applications reported in the literature for hydrological and water resources assessment, in the water quantity aspects (water discharge, groundwater dynamics, soil water, snow dynamics, and water management), water quality assessment (land-use and land-management change, best management practices in agriculture), and climate change impact. And several authors have also written reviews about the application of SWAT model (Arnold and Fohrer 2005; Gassman et al. 2007; Krysanova and Arnold 2008).

Calibration and validation

The application of the model first involved the analysis of parameter sensitivity, which was then used for model calibration (Muleta and Nicklow 2005). The calibration was carried out with combined auto and manual calibration using flow data from January 2000 to December 2004. For the streamflow and non-point source pollutant load simulation, manual calibration was performed for monthly time steps using measurements from the Shitoukoumen gauging station at the catchment outlet.

The goodness-of-fit measures used were the coefficient of determination (R^2 ; Eq. (1)) and the Nash–

Sutcliffe efficiency (E_{NS} , (Eq. (2)) (Nasha and Sutcliffea 1970). The R^2 and E_{NS} values are explained in Eqs. 1 and 2:

$$R^2 = \frac{(\sum_{i=1}^n (O_i - \bar{O})(P_i - \bar{P}))^2}{\sum_{i=1}^n (O_i - \bar{O})^2 \sum_{i=1}^n (P_i - \bar{P})^2} \tag{1}$$

$$E_{NS} = \frac{\sum_{i=1}^n (O_i - \bar{O})^2 - \sum_{i=1}^n (P_i - O_i)^2}{\sum_{i=1}^n (O_i - \bar{O})^2} \tag{2}$$

where P_i are the model-predicted values, O_i are the observed values, and \bar{O} is the mean of observed values. The optimal statistical value occurs when the R^2 and E_{NS} values are closest to 1.

Surface runoff was calibrated until average measured and simulated values were within 15% of each other, monthly $R^2 > 0.6$, and $E_{NS} > 0.5$. Organic and mineral nitrogen and phosphorus were calibrated to within 25% after flow calibration was completed (Santhi et al. 2001). A value greater than 0.75 for monthly E_{NS} can be considered very good; between 0.65 and 0.75 can be considered good, while its value between 0.5 and 0.65 is considered satisfactory (Moriassi et al. 2007)

After model calibration was finished, model validation followed. Model validation is the process of performing the simulation using data collected from January 2005 to December 2007, without changing any parameter values that may have been adjusted during calibration.

Results and discussion

Generation of future climate data

The structure and operation of SDSM include the following five distinct tasks (Wilby et al. 2002): (1) screening of predictor variables, (2) model calibration, (3) synthesis of measurement data, (4) generation of climate change scenarios, and (5) diagnostic testing and statistical analyses.

Selecting predictors

In SDSM, the selection of the most relevant predictor variables was carried out through linear correlation analysis, partial correlation analysis, and scatter plots

between the predictors and the predictand variables. Large-scale predictor variables representing the current climate conditions, derived from the NCEP reanalysis data sets, were used to investigate the percentage of variance explained by each predictand–predictor pair. The predictors that had reasonable correlations with the measured daily maximum and minimum temperature and precipitation were selected from the NCEP/NCAR variables and listed in Table 1.

Calibration and validation of SDSM

Model calibration in this case was to find the coefficients of the multiple linear regression equation parameters that relate the large-scale atmospheric variables derived from the NCEP data set and local-scale variables. The calibration period for temperature and precipitation was from 1961 to 1975, and the validation period was 1976–1990. The calibration and validation results are shown in Table 2.

As is shown in Table 2, 73.8% and 75% of the variance in maximum and minimum air temperature could be explained by the downscaling model, while only 16.6% of the variance in daily precipitation could be explained. The relative errors for T_{max} , T_{min} , and daily precipitation were 0.8%, 3.9%, and 3.7% in the calibration period. The relatively low explained variance for daily precipitation is consistent with previous studies and underlines the difficulty of downscaling local precipitation series from regional-scale predictors. Presently, the unexplained component in daily precipitation amounts is generally treated stochastically by the downscaling model.

Figure 2 shows the performance of the model during the validation period. The graph shows a good agreement between the observed and simulated mean daily maximum and minimum temperatures for all months of the year. However, the daily average precipitation was overestimated. Unlike temperature, precipitation is a conditional process that depends on other intermediate processes such as humidity, cloud cover, and whether a day is wet or dry. For that reason, precipitation is identified by many researchers as one of the most problematic variables in downscaling. For the validation period, the relative errors for T_{max} , T_{min} , and daily precipitation were 9.1%, 12.9%, and 5.8%. The statistical relationship established by using SDSM is suitable for the generation of future climate change scenarios.

Table 1 Large-scale climate predictors for computing surface meteorological variables with SDSM model

Predictand	T_{\max}	T_{\min}	PRCP
Predictor	mssl (mean sea level pressure)	mssl (mean sea level pressure)	p500 (geopotential height at 500 hPa)
	p_z (surface vorticity)	p_z (surface vorticity)	p8_z (vorticity at 850 hPa)
	p500 (geopotential height at 500 hPa)	p_v (surface zonal wind)	r500 (relative humidity at 500 hPa)
	p8_z (vorticity at 850 hPa)	p8_z (vorticity at 850 hPa)	r850 (relative humidity at 850 hPa)
	p850 (geopotential height at 850 hPa)	p850 (geopotential height at 850 hPa)	shum (near surface specific humidity)
		shum (near surface specific humidity)	

Results for future climate change

The SDSM model, after sufficient calibration and validation, was used to downscale the GCM (HadCM3) outputs to generate future climate change scenarios. It can be seen from Fig. 3 that there is a general increasing trend for both minimum and maximum temperature in the A2 scenario for the three future periods and that the degree of increase of the daily minimum temperature is smaller than that of the daily maximum temperature. Compared with baseline data of 1961–1990, the maximum temperature would increase by an average of 1.67°C, 3.44°C, and 5.65°C in the 2020s, 2050s, and 2080s, respectively, and the minimum temperature would increase by an average of 1.07°C, 2.68°C, and 4.69°C. The monthly changes of minimum and maximum temperatures for the future showed heterogeneity. The temperature showed significant increasing trends in most months, showing slight decreases only in April and May in the 2020s. The average daily precipitation showed a significant increasing trend in most months, especially in September, and slight decreases in April to June. Compared with the baseline of 1961–1990, the daily precipitation increased by an average of 1.12, 0.89, and 1.72 mm in July, August, and

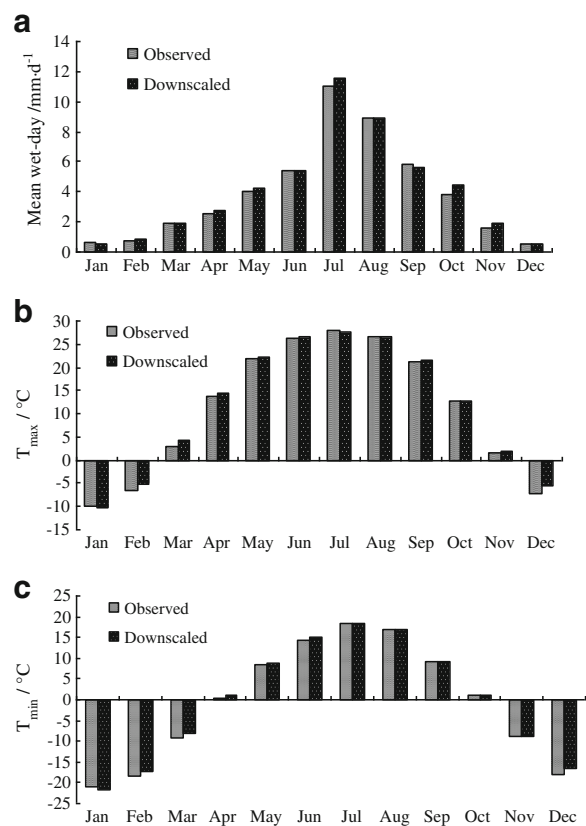
Table 2 Explained variances, standard errors, and relative error for maximum and minimum air temperature and daily precipitation between observed and simulated results in the calibration period (1961–1975) and the validation period (1976–1990)

Predictant	Calibration		Validation
	E%	Er	Er
T_{\max} (°C)	73.8	0.008	0.091
T_{\min} (°C)	75.0	0.039	0.129
Precipitation (mm)	16.6	0.037	0.058

September in the three future periods. The daily temperature and precipitation all showed a sharp increase from July to September.

Characteristics analysis for future climate change

The characteristics of future climate change of the Shitoukoumen reservoir catchment were further analyzed using the linear regression and Mann–

**Fig. 2** Comparison between average daily precipitation (a), maximum (b), and minimum (c) air temperature per month in study area during validation (1976–1990)

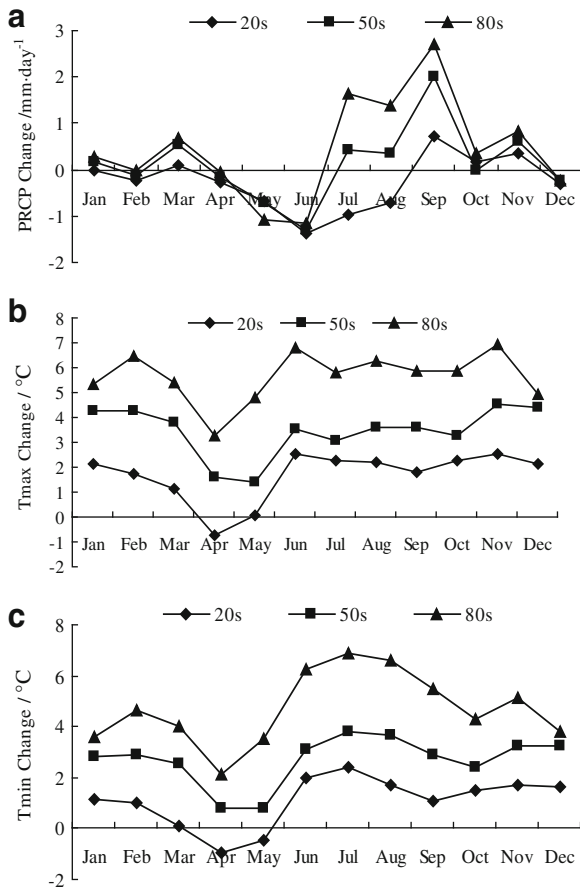


Fig. 3 Monthly average of daily precipitation, maximum and minimum temperature in the present study during the three future periods compared with the baseline data of 1961–1990

Kendall trend analysis methods. The Mann–Kendall (M–K) test method is widely used to detect trends in hydroclimatic time series (Chen et al. 2007; Pellicciotti et al. 2007).

Figure 4 shows the simulated annual average precipitation and temperature curves, the 5-year moving average curves, and the linear regression curves. The daily mean temperature shows a fluctuating upward trend in future periods with two minimum values, in 2070 and 2065, and subsequently a steady rise from 2070 to 2099. For annual precipitation, there is also an increasing trend with annual fluctuations. The precipitation shows a downward trend in 2010–2040 toward a less rainy period and a subsequent upward trend in 2040–2060 toward a more rainy period. Then, there are upward and downward trends with slight fluctuations from 2060 to 2090, followed by an increasing trend after 2090 toward a more rainy period.

Table 3 lists the values of the regression slope b , the Z_c values obtained from M–K test methods, and Kendall slope β value. It can be seen that the warming trends of average annual and seasonal daily temperature were all significant at the >95% confidence level, and β values were all positive numbers, which shows that this upward trend is obvious. The increase degrees of the four seasons are similar. The climatic change rate of annual mean temperature is 0.63°C per decade. Annual precipitation also shows an increasing trend, though it is not statistically significant at the >95% confidence level, and climatic change rate reaches 11 mm per decade. For the seasonal change, precipitation was significantly decreased in spring, while it showed a significantly increasing trend in summer and winter. Compared to other seasons, the summer precipitation and temperature make the largest contribution to the increase in annual precipitation and temperature. So, the future precipitation and temperature will have significant changes in summer.

The response of non-point source pollutant loads to climate change

SWAT model calibration and validation

Parameter sensitivity analysis was performed before the calibration and validation of the SWAT model.

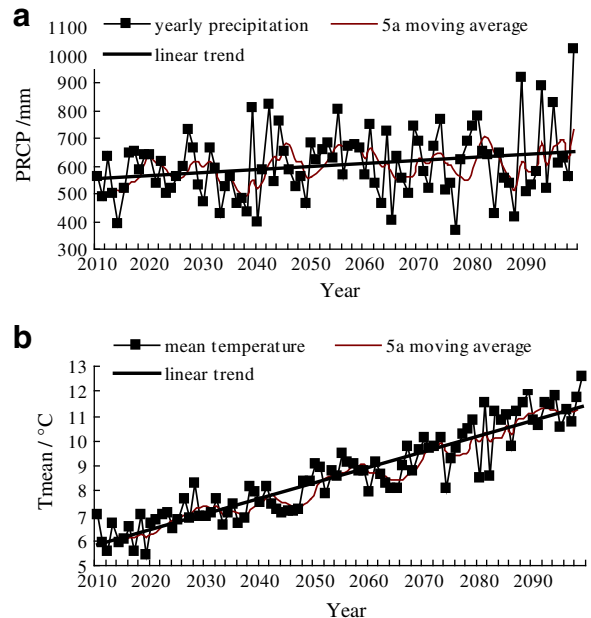


Fig. 4 The annual average temperature, precipitation characteristic curve in study area in the future period (2010–2099)

Table 3 Results of the trend test for the series of daily mean temperature and precipitation

	T_{mean}				Precipitation			
	b ($^{\circ}\text{C}/10\text{a}$)	Z_c	H_0	β	b (mm/10a)	Z_c	H_0	β
Annual	0.63	10.73*	Reject	0.064	11	1.75	Accept	0.805
Spring	0.6	7.79*	Reject	0.063	-2.15	-2.36*	Reject	-0.231
Summer	0.72	9.52*	Reject	0.071	12.7	2.40*	Reject	1.057
Autumn	0.59	9.08*	Reject	0.059	-0.25	-0.25	Accept	-0.049
Winter	0.55	7.68*	Reject	0.055	0.6	2.92*	Reject	0.043
Dry seasons	0.57	8.65*	Reject	0.056	0.99	1.04	Accept	0.079
Rainy seasons	0.69	10.67*	Reject	0.069	9.93	1.74	Accept	0.734

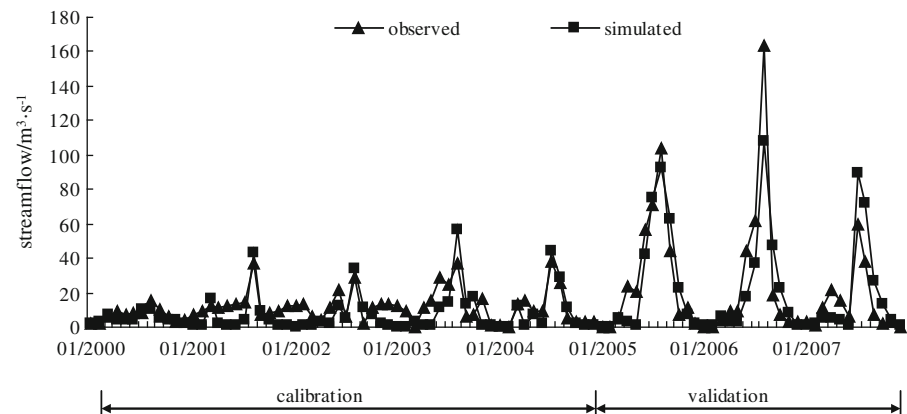
* $p < 0.05$

Sensitive parameters identified by an autocalibration–sensitivity analysis procedure embedded in SWAT version 2005 included CN2 (curve number), soil evaporation compensation factor, soil available water capacity, and base flow alpha factor.

The calibration was carried out with an auto mode combined with manual adjustment of sensitive parameters using flow data from January 1, 2000, to December 31, 2004. Because the nutrient loss data for 2000–2005 were not available, model performance was evaluated through calibration for 2006 with $\text{NH}_4^+\text{-N}$ data and validation for 2007 with both $\text{NH}_4^+\text{-N}$ and total phosphorus (TP) data.

Figures 5 and 6 show the comparisons of the monthly measured and simulated stream flows and $\text{NH}_4^+\text{-N}$ and TP loads during both the calibration and validation periods at the Shitoukoumen reservoir inlet. Except for some years during which simulated peaks are greater than observed ones or peak flows are underestimated, most of the periods show a very good agreement between the simulated and observed

streamflows, and the observed and simulated values plotted near the 1:1 line. The statistical evaluations for streamflow showed that E_{NS} and R^2 values were 0.76 and 0.78 in calibration and 0.71 and 0.74 in validation, further confirming that the model captured the monthly measured trends. Distribution of the observed and simulated values of $\text{NH}_4^+\text{-N}$ and TP load along with the 1:1 lines are presented in Figs. 7a, b and 8. It revealed that the simulated values of $\text{NH}_4^+\text{-N}$ and TP were in close agreement with the observed values. The values of R^2 and E_{NS} for the $\text{NH}_4^+\text{-N}$ calibration were 0.72 and 0.68, and the values were 0.71 and 0.65 for the model validation. The values of R^2 and E_{NS} for TP were 0.74 and 0.63 for the model validation. The relative errors for observed and simulated streamflow and $\text{NH}_4^+\text{-N}$ and TP loads were within the evaluation criteria. The values of the statistical parameters indicate that the SWAT model was successful in assessing streamflow and $\text{NH}_4^+\text{-N}$ and TP loads for the entire catchment.

Fig. 5 Simulated and measured monthly streamflow at the Shitoukoumen gauging station (E_{NS} of 0.76 for the calibration period, 0.71 for the validation period)

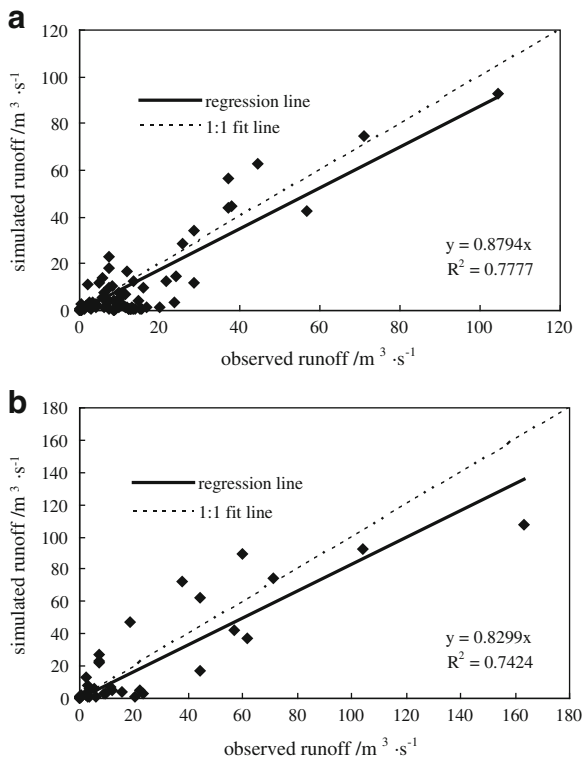


Fig. 6 Comparison between observed and simulated streamflow for model calibration (a) and validation (b)

Impact of climate change on streamflow and non-point source pollution in Shitoukoumen reservoir catchment

To assess the impact of global warming on streamflow and non-point source pollution in the Shitoukoumen reservoir catchment, daily precipitation and temperature series obtained from a GCM (HadCM3) grid were as input to the SWAT model. It is seen from Fig. 9 that there is insignificant change of streamflow or NH₄⁺-N and TP loads from January to May in the three periods. The future monthly streamflow will increase by an average of 18.5 m³/s from September to December in the three future periods compared with the baseline data of 1961–1990. The NH₄⁺-N load entering the reservoir increases significantly in September by an average of 137.7, 60.3, and 36.6 t, respectively, in the 2020s, 2050s, and 2080s compared with baseline data, and the TP load increases significantly in July by an average of 63.6 and 149.7 t in the 2050s and 2080s. It can be seen that there are similar changes in streamflow and NH₄⁺-N and TP loads from January to September. They all showed

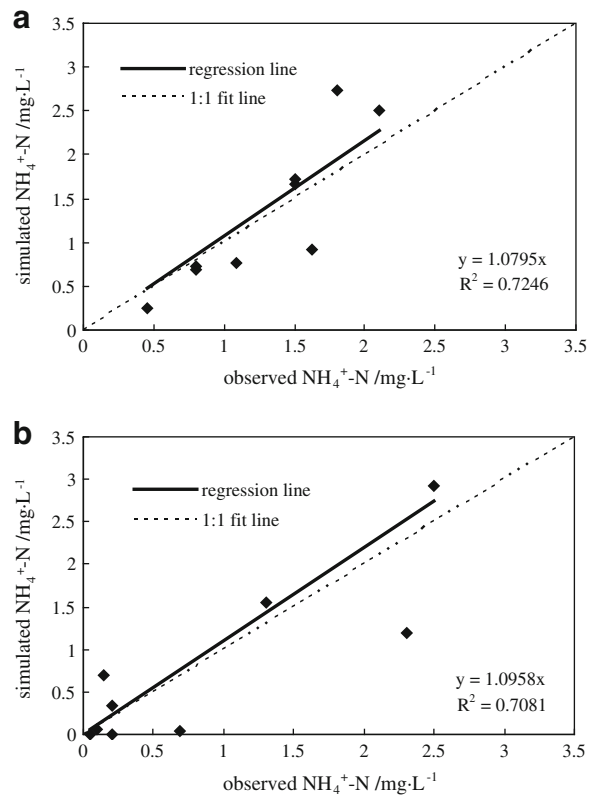


Fig. 7 Comparison between observed and simulated NH₄⁺-N concentration from inlet of Shitoukoumen reservoir for model calibration (a) and validation (b)

slight or no change from January to June and then a sharp increase in July and September. The streamflow continued to increase from October to December, while NH₄⁺-N and TP loads showed no changes. The variations may be due to the agricultural management

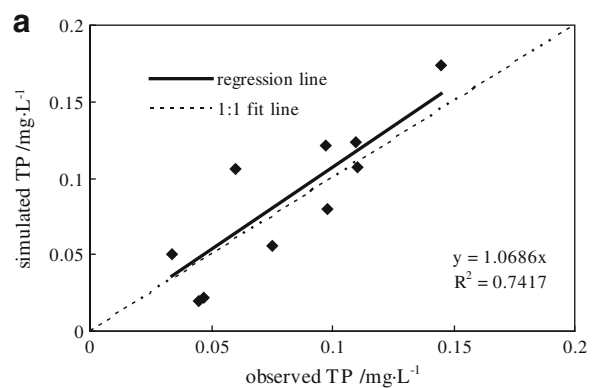


Fig. 8 Comparison between observed and simulated total phosphorus concentration from inlet of Shitoukoumen reservoir for model validation (a)

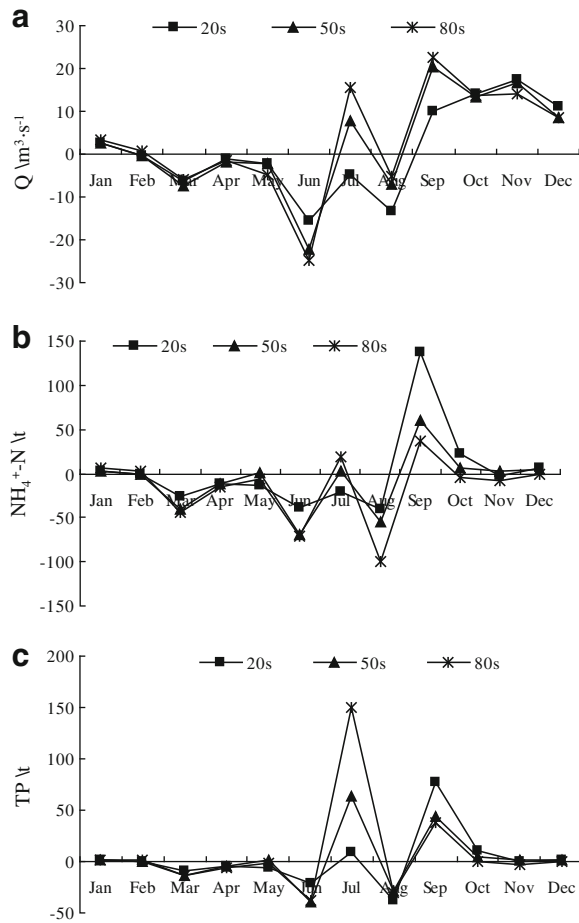


Fig. 9 The monthly response of streamflow, $\text{NH}_4^+\text{-N}$, and TP load change compared with the average streamflow, $\text{NH}_4^+\text{-N}$, and TP load from 1961 to 1990

practices. To investigate the correlations between streamflow and nutrient loads, the SPSS statistical software was used. The results reveal that $\text{NH}_4^+\text{-N}$ and TP loads have positive correlations with streamflow (correlation coefficients of 0.68 and 0.684, respectively, at 95% confidence level). The non-point source pollutant loads have similar trends to that of streamflow, indicating that runoff plays a decisive role in the changes of pollutant concentrations.

Characteristics analysis for future streamflow and non-point source pollutant loads change

Long-term trends in the annual and seasonal streamflow and non-point source pollutant loads of Shitoukoumen reservoir catchment were tested by linear regression and Mann–Kendall methods. Figure 10 shows the simulated

annual streamflow and $\text{NH}_4^+\text{-N}$ and TP loads. The streamflow shows fluctuating upward trends from 2010 to 2099. The 5-year moving average curve indicates that annual streamflow shows the following trends: an upward trend from 2010 to 2022, a downward trend from 2022 to 2040, a sharp increase from 2040 to 2062, a slowly declining trend from 2062 to 2078, sharp upward and downward trends in 2082 and 2088, respectively, and an increasing trend from 2088 to 2099. For the $\text{NH}_4^+\text{-N}$ load, there are two significant fluctuating upward and downward trends, from 2042 to 2048 and from 2070 to 2078, with only slight fluctuations in other years. The variations in TP load are very similar to those of the $\text{NH}_4^+\text{-N}$ load, with significant peak values in 2046 and 2075.

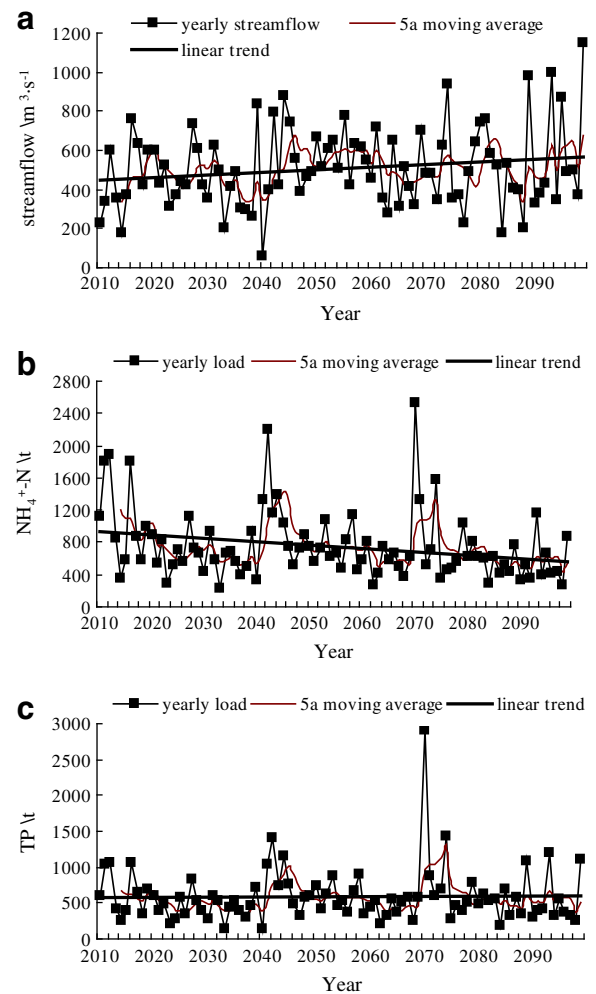


Fig. 10 The annual average streamflow (a), $\text{NH}_4^+\text{-N}$ (b), and TP (c) load characteristic curve in study area in the future period (2010–2099)

Table 4 Results of the trend test for the series of streamflow

	Streamflow			
	b ($m^3 s^{-1}/10a$)	Z_c	H_0	β
Annual	1.1	1.07	Accept	0.881
Spring	-0.08	-1.98*	Reject	-0.059
Summer	1.32	2.08*	Reject	0.942
Autumn	0.15	0.06	Accept	0.025
Winter	0.05	0.03	Accept	0.002
Dry seasons	-0.04	-0.55	Accept	-0.088
Rainy seasons	1.43	1.28	Accept	0.940

* $p < 0.05$

The values of the regression slope b , the significant level, and the Mann–Kendall statistics Z_c and β values are listed in Table 4 and Table 5. According to the M–K statistics: $|Z_c| > Z_{1-p/2} = 1.96$, streamflow shows a significant downward trend in spring ($\beta < 0$) and an upward trend in summer ($\beta > 0$) at the $p = 0.05$ significance level. However, the changes in trend of annual and other seasonal streamflows are not significant. The b values indicate annual streamflow increase by $1.1 m^3 s^{-1}$ per decade, and the rates of seasonal streamflow change (in cubic meters per-second per decade) are -0.08 in spring, 1.32 in summer, 0.15 in autumn, 0.05 in winter, -0.04 in dry seasons, and 1.43 in rainy seasons. The contribution to annual streamflow in summer is larger than it is in other seasons, so measures to prevent the occurrence of flood disaster need to be considered. As for the NH_4^+ -N load into the reservoir, the decreasing trend is significant in all periods except summer and winter. The rates of annual and seasonal change in NH_4^+ -N load are (in tons per decade): -40.6 annually, -2.526

in spring, 1.434 in summer, -9.481 in autumn, -0.095 in winter, -1.145 in dry seasons, and -5.623 in rainy seasons. Compared with other seasons, the decreasing trend of NH_4^+ -N load in autumn contributes the most to the decrease of annual load. The TP load into the reservoir shows a significant downward trend in spring and dry seasons by $\beta < 0$, and Z_c values are -2.15 and -2.942 , respectively. The annual TP load shows an increasing, though not statistically significant, trend, and its rate of variation is 3.77 t per decade. The rates of seasonal TP load change (in tons per decade) are -2.15 in spring, 6.335 in summer, -4.2 in autumn, -0.015 in winter, -0.343 in dry seasons, and 0.971 in rainy seasons. The upward trend of TP load in summer contributes the most to the increase of annual load compared with other seasons. These loads may cause further deterioration of the water quality of Shitoukoumen reservoir.

Conclusions

In this study, the effects of potential climate change on streamflow volume and NH_4^+ -N and TP load in the inlet of the Shitoukoumen Reservoir were analyzed based on projected climate change conditions developed using the SDSM combined with GCM output and a complex, physically based, distributed hydrologic model (SWAT). The following main conclusions are drawn:

- (1) The SWAT model was successfully applied in the inlet of Shitoukoumen Reservoir through observation data. The statistical evaluations for streamflow show that the E_{NS} and R^2 values were 0.71 and 0.74 in validation. Values of R^2 for NH_4^+ -N calibration and validation were 0.72

Table 5 Results of the trend test for the series of NH_4^+ -N and TP load

	NH_4^+ -N				TP			
	b (t/10a)	Z_c	H_0	β	b (t/10a)	Z_c	H_0	β
Annual	-40.6	-2.86*	Reject	-3.554	3.77	-0.36	Accept	-0.368
Spring	-2.52	-3.51*	Reject	-0.151	-2.15	-3.17*	Reject	-0.058
Summer	-1.43	-0.79	Accept	-0.276	6.33	0.94	Accept	0.289
Autumn	-9.48	-2.51*	Reject	-0.382	-4.23	-1.86	Accept	-0.164
Winter	-0.09	-0.52	Accept	-0.011	-0.02	-0.33	Accept	-0.002
Dry seasons	-1.14	-3.19*	Reject	-0.098	-0.34	-2.94*	Reject	-0.032
Rainy seasons	-5.62	-2.51*	Reject	-0.521	0.97	-0.20	Accept	-0.037

* $p < 0.05$

and 0.71, respectively, and R^2 was 0.74 for TP in model validation. The evaluation results showed that the SWAT model was able to simulate well the monthly streamflow and $\text{NH}_4^+\text{-N}$ and TP loads.

- (2) The SDSM, which was calibrated and validated using the NCEP reanalysis data sets and observational data, could well downscale GCM (HadCM3) output to generate climate change from 2010 to 2099 in the A2 scenario. The projected daily temperature showed a significant increase of 0.63°C per decade. Annual precipitation also shows an increasing trend of 11 mm per decade, but the differences are not statistically significant. Precipitation shows its most significant increase in summer, by 12.70 mm per decade, which makes the largest contribution to the increase in annual precipitation compared to other seasons.
- (3) The simulated future climate change values were used as input for the SWAT model. The annual streamflow shows upward trends from 2010 to 2099, with an increase of $1.1 \text{ m}^3 \text{ s}^{-1}$ per decade, and a significant downward trend in spring and an upward trend in summer. The increase rate of streamflow in summer reaches $1.32 \text{ m}^3 \text{ s}^{-1}$ per decade. The annual $\text{NH}_4^+\text{-N}$ load into the reservoir shows a significant downward trend of 40.6 t per decade. Compared with other seasons, the decreasing trend of $\text{NH}_4^+\text{-N}$ load in autumn contributes the most to the decrease of annual load. The annual TP load shows an increasing, but not statistically significant, trend of 3.77 t per decade. The increasing rate of TP load in summer reaches 6.335 t per decade, which contributes the most to the increase of annual load compared with other seasons. The $\text{NH}_4^+\text{-N}$ and TP loads also have positive correlations with streamflow.
- (4) In general, streamflow volume and TP load in the study area are predicted to experience dramatic changes in the future. Although the projected changes in climate, streamflow, and non-point source pollutant loads through GCMs combined with the SWAT model cannot be projected exactly because of the uncertainty in climate change scenarios and GCM outputs, the general results of this analysis should be identified and incorporated into water resources management

plans and water quality remediation. The development of a higher spatial and temporal resolution of the GCMs and coupling of hydrological model will be essential to further studies.

Acknowledgment This research was supported by major projects on control and rectification of water body pollution (no. 2009ZX07526-006-04-01). Project 20101060 was supported by the Graduate Innovation Fund of Jilin University. Key Laboratory of Groundwater Resources and Environment of Ministry of Education are all gratefully acknowledged.

References

- Arnold, J. G., & Fohrer, N. (2005). SWAT2000: current capabilities and research opportunities in applied watershed modelling. *Hydrological Processes*, 19(3), 563–572.
- Arnold, J. G., Srinivasan, R., Muttiyah, R. S., & Williams, J. R. (1998). Large area hydrologic modeling and assessment part I: model development. *Journal of the American Water Resources Association*, 34, 73–89.
- Bates, B. C., Hope, P., Ryan, B., Smith, I., & Charles, S. (2008). Key findings from the Indian Ocean Climate Initiative and their impact on policy development in Australia. *Climatic Change*, 89(3–4), 339–354.
- Campbell, J. L., Rustad, L. E., Boyer, E. W., Christopher, S. F., Driscoll, C. T., Fernandez, I. J., et al. (2009). Consequences of climate change for biogeochemical cycling in forests of northeastern North America. *Canadian Journal of Forest Research-Revue Canadienne De Recherche Forestiere*, 39(2), 264–284.
- Chen, H., Guo, S., Xu, C.-Y., & Singh, V. P. (2007). Historical temporal trends of hydro-climatic variables and runoff response to climate variability and their relevance in water resource management in the Hanjiang basin. *Journal of Hydrology*, 344(3–4), 171–184.
- Chu, J. T., Xia, J., Xu, C. Y., & Singh, V. P. (2009). Statistical downscaling of daily mean temperature, pan evaporation and precipitation for climate change scenarios in Haihe River, China. *Theoretical and Applied Climatology*, 99(1–2), 149–161.
- Delpa, I., Jung, A. V., Baures, E., Clement, M., & Thomas, O. (2009). Impacts of climate change on surface water quality in relation to drinking water production. *Environment International*, 35(8), 1225–1233.
- Di Luzio, M., Srinivasan, R., & Arnold, J. G. (2004). A GIS-coupled hydrological model system for the watershed assessment of agricultural nonpoint and point sources of pollution. *Transactions in GIS*, 8(1), 113–136.
- Diaz-Nieto, J., & Wilby, R. L. (2005). A comparison of statistical downscaling and climate change factor methods: impacts on low flows in the River Thames, United Kingdom. *Climatic Change*, 69(2–3), 245–268.
- Dibike, Y. B., & Coulibaly, P. (2005). Hydrologic impact of climate change in the Saguenay watershed: comparison of downscaling methods and hydrologic models. *Journal of Hydrology*, 307(1–4), 145–163.

- Fowler, H. J., Blenkinsop, S., & Tebaldi, C. (2007). Linking climate change modelling to impacts studies: recent advances in downscaling techniques for hydrological modelling. *International Journal of Climatology*, 27(12), 1547–1578.
- Gassman, P. W., Reyes, M. R., Green, C. H., & Arnold, J. G. (2007). The soil and water assessment tool: historical development, applications, and future research directions. *Transactions of the ASABE*, 50(4), 1211–1250.
- Ghosh, S., & Mujumdar, P. (2008). Statistical downscaling of GCM simulations to streamflow using relevance vector machine. *Advances in Water Resources*, 31(1), 132–146. doi:10.1016/j.advwatres.2007.07.005.
- Githui, F., Mutua, F., & Bauwens, W. (2009). Climate change impact on SWAT simulated streamflow in western Kenya. *International Journal of Climatology*, 29(12), 1823–1834.
- Graham, L. P., Andreasson, J., & Carlsson, B. (2007). Assessing climate change impacts on hydrology from an ensemble of regional climate models, model scales and linking methods—a case study on the Lule River basin. *Climatic Change*, 81, 293–307.
- Graiprab, P., Pongput, K., Tangtham, N., & Gassman, P. W. (2010). Hydrologic evaluation and effect of climate change on the At Samat watershed, Northeastern Region, Thailand. *International Agricultural Engineering Journal*, 19(2), 12–22.
- Hamlet, A. F., & Lettenmaier, D. P. (1999). Effects of climate change on hydrology and water resources in the Columbia River basin. *Journal of the American Water Resources Association*, 35(6), 1597–1623.
- Hodgkins, G. A., Dudley, R. W., & Huntington, T. G. (2003). Changes in the timing of high river flows in New England over the 20th century. *Journal of Hydrology*, 278(1–4), 244–252.
- Jha, M. K. (2004). *Hydrologic modeling and climate change study in the Upper Mississippi River Basin using SWAT*. Ames: Iowa State University.
- Kendall, M. G. (1975). *Rank correlation methods*. London: Griffin.
- Krysanova, V., & Arnold, J. G. (2008). Advances in ecohydrological modelling with SWAT—a review. *Hydrological Sciences Journal—Journal Des Sciences Hydrologiques*, 53(5), 939–947.
- Lee, E., Seong, C., Kim, H., Park, S., & Kang, M. (2010). Predicting the impacts of climate change on nonpoint source pollutant loads from agricultural small watershed using artificial neural network. *Journal of Environmental Sciences*, 22(6), 840–845.
- Limaye, A. S., Boyington, T. M., Cruise, J. F., Bulus, A., & Brown, E. (2001). Macroscale hydrologic modeling for regional climate assessment studies in the southeastern United States. *Journal of the American Water Resources Association*, 37(3), 709–722.
- Mann, H. B. (1945). Nonparametric tests against trend. *Econometrica*, 13, 245–259.
- Moriasi, D., Arnold, J., Van Liew, M., Bingner, R., Harmel, R., & Veith, T. (2007). Model evaluation guidelines for systematic quantification of accuracy in watershed simulations. *Transactions of ASAE*, 50(3), 885–900.
- Muleta, M. K., & Nicklow, J. W. (2005). Sensitivity and uncertainty analysis coupled with automatic calibration for a distributed watershed model. *Journal of Hydrology*, 306(1–4), 127–145.
- Murdoch, P. S., Baron, J. S., & Miller, T. L. (2000). Potential effects of climate change on surface water quality in North America. *Journal of American Water Resources Association*, 36, 347–366.
- Nasha, J. E., & Sutcliffe, J. V. (1970). River flow forecasting through conceptual models: part I—a discussion of principles. *Journal of Hydrology*, 10, 282–290.
- Neff, R., Chang, H. J., Knight, C. G., Najjar, R. G., Yarnal, B., & Walker, H. A. (2000). Impact of climate variation and change on Mid-Atlantic Region hydrology and water resources. *Climate Research*, 14(3), 207–218.
- Neitsch, S. L., Arnold, J. G., Kiniry, J. R., & Williams, J. R. (2005). *Soil and water assessment tool theoretical documentation version 2005*. Temple: Grassland, Soil and Water Research Laboratory.
- Park, J.-H., Duan, L., Kim, B., Mitchell, M. J., & Shibata, H. (2010). Potential effects of climate change and variability on watershed biogeochemical processes and water quality in Northeast Asia. *Environment International*, 36(2), 212–225.
- Payne, J. T., Wood, A. W., Hamlet, A. F., Palmer, R. N., & Lettenmaier, D. P. (2004). Mitigating the effects of climate change on the water resources of the Columbia River Basin. *Climatic Change*, 62(1–3), 233–256.
- Pellicciotti, F., Burlando, P., & van Vliet, K. (2007). Recent trends in precipitation and streamflow in the Aconcagua River basin, central Chile. *IAHS Publications*, 318, 17–38.
- Randall, D. A., Wood, R. A., Bony, S., Colman, R., Fichet, T., Fyfe, J., et al. (2007). Climate models and their evaluation. In S. Solomon, D. Qin, M. Manning, Z. Chen, M. Marquis, & K. B. Averyt (Eds.), *Climate change 2007: the physical science basis. Contribution of Working Group I to the Fourth Assessment Report of the Intergovernmental Panel on Climate Change* (pp. 598–662). Cambridge: Cambridge University Press.
- Santhi, G., Arnold, J. G., Williams, J. R., Dugas, W. A., Srinivasan, R., & Hauck, L. M. (2001). Validation of the SWAT model on a large river basin with point and nonpoint sources. *Journal of American Water Resources Association*, 37(6), 1169–1188.
- Stone, M. C., & Hotchkiss, R. H. (2003). Water yield responses to high and low spatial resolution climate change scenarios in the Missouri River Basin. *Geophysical Research Letters*, 30(4), 1186.
- Stone, M. C., Hotchkiss, R. H., Hubbard, C. M., Fontain, E. T. A., Mearns, L. O., & Arnold, J. G. (2001). Impacts of climate change on Missouri River Basin water yield. *Journal of the American Water Resources Association*, 37(5), 1119–1299.
- Tu, J. (2009). Combined impact of climate and land use changes on streamflow and water quality in eastern Massachusetts, USA. *Journal of Hydrology*, 379(3–4), 268–283.
- Whitehead, P. G., Wilby, R. L., Butterfield, D., & Wade, A. J. (2006). Impacts of climate change on in-stream nitrogen in a lowland chalk stream: an appraisal of adaptation strategies. *Science of the Total Environment*, 365(1–3), 260–273.
- Wikipedia (2011). NCEP/NCAR reanalysis. http://en.wikipedia.org/wiki/NCEP/NCAR_Reanalysis Accessed 19 May 2011.
- Wilby, R. L., Dawson, C. W., & Barrow, E. M. (2002). SDSM—a decision support tool for the assessment of regional climate change impacts. *Environmental Modelling and Software*, 17(2), 147–159.

- Williamson, C. E., Dodds, W., Kratz, T. K., & Palmer, M. A. (2008). Lakes and streams as sentinels of environmental change in terrestrial and atmospheric processes. *Frontiers in Ecology and the Environment*, 6(5), 247–254.
- Xu, C. Y. (1999). Climate change and hydrologic models: a review of existing gaps and recent research developments. *Water Resources Management*, 13(5), 369–382.
- Xu, Z. X., Zhao, F. F., & Li, J. Y. (2009). Response of streamflow to climate change in the headwater catchment of the Yellow River basin. *Quaternary International*, 208, 62–75.
- Yu, P. S., Yang, T. C., & Wu, C. K. (2002). Impact of climate change on water resources in southern Taiwan. *Journal of Hydrology*, 260(1–4), 161–175.
- Zhang, X., Srinivasan, R., & Hao, F. (2007). Predicting hydrologic response to climate change in the Luohe River basin using the SWAT model. *Transactions of the ASABE*, 50(3), 901–910.